Report No. FRA-OR&D 75-30

FRAGMENTATION AND METALLURGICAL ANALYSIS OF TANK CAR RAX 201

Charles Anderson
E.B. Norris

APRIL 1974
FINAL REPORT

Prepared For
U.S. DEPARTMENT OF TRANSPORTATION
FEDERAL RAILROAD ADMINISTRATION
Office of Research, Development, and Demonstrations
Washington, D.C. 20590

NOTICE

Technical Report Documentation Page

1. Report No.	2. Government Accession No.	3. Recipient's Catalog No.
FRA-OR&D 75-30		

4. Title and Subtitle	5. Report Date
FRAGMENTATION AND METALLURGICAL ANALYSIS OF TANK CAR RAX 201	April 1974
	6. Performing Organization Code
	- -
7. Author(s)	8. Performing Organization Report No.
Charles Anderson; E.B. Norris	
9. Performing Organization Name and Address	10. Work Unit No. (TRAIS)
U.S. Department of the Army Ballistic Research Laboratories Aberdeen Proving Ground, Maryland	11. Contract or Grant No. DOT-AR-30026
	13. Type of Report and Period Covered
12. Sponsoring Agency Name and Address	FINAL REPORT
U.S. Department of Transportation Federal Railroad Administration Office of Research, Development and Demonstrations Washington, D.C. 20590	14. Sponsoring Agency Code

15. Supplementary Notes

16. Abstract

On 28 July 1973, the Ballistic Research Laboratories performed a full-scale fire test on a 33,000 gallon, DOT 112A340W non-insulated, pressure, rail tank car for the Federal Railroad Administration and Association of American Railroads. The car was filled with liquified petroleum gas (LPG). After 24.5 minutes of exposure to the fire, the tank car ruptured. This report concerns the mapping of the fragments and metallurgical analysis of the ruptured car, along with an investigation of the cause and initial location of failure.

17. Key Words	18. Distribution Statement
Liquefied Petroleum gases, fire research, tank cars	Document is available to the public through the National Technical Information Service, Springfield, Virginia 22161

19. Security Classif. (of this report)	20. Security Classif. (of this page)	21. No. of Pages	22. Price
Unclassified	Unclassified	41	-

Form DOT F 1700.7 (8-72) Reproduction of completed page authorized

TABLE OF CONTENTS

LIST OF TABLES

LIST OF FIGURES

I. INTRODUCTION

The Ballistic Research Laboratories (BRL), at the request of the Federal Railroad Administration of the Department of Transportation (FRA/DOT), have been investigating the effects of large, intense pool fires on pressurized railroad tank cars filled with hazardous materials. This effort is part of an extensive research program, jointly sponsored by FRA/DOT and Railway Progress Institute - Association of American Railroads (RPI-AAR), designed to develop methods to minimize personal injury and property damage due to the rupture of railroad tank cars filled with flammable materials.

On 28 July 1973, a fire test was performed on a rail tank car at White Sands Missile Range (WSMR), New Mexico. The tank car was filled with approximately 125 kiloliters (33,000 gallons) of liquified petroleum gas (LPG). Twenty-four and one-half minutes of exposure to an intense hydrocarbon fire resulted in the car rupturing. Another BRL report currently being published goes into detail concerning the mechanics of the experiment, and the collection and presentation of the data gathered. This report investigates some of the aspects of the rupturing; much of the work presented here was performed by Southwest Research Institute (SwRI), San Antonio, Texas.

II. BACKGROUND ON THE TANK CAR AND TEST PROCEDURES

The procedure consisted of simulating a possible accident environment. Fire engulfment, whether the result of a derailment and puncture, coupler puncture, or a previous rupture, is one of the more severe conditions to which a rail tank car can be subjected. For this test, a full size railroad tank car was positioned in a large excavation and filled with LPG. The energy for the external fire was provided by a pool of JP-4 jet fuel situated beneath the tank car.

The tank car, RAX 201, was especially built for the test; the main differences between RAX 201 and a normal rail tank car of the 33,000 gallon, DOT 112A340W non-insulated pressure tank car series, were the inclusion of a second entranceway (manway) to the interior of the tank and two ports through which instrumentation lines could be run. Otherwise, RAX 201 met all applicable requirements of the U. S. Department of Transportation and the Association of American Railroads. RAX 201, except for the few changes to facilitate instrumentation, was a standard tank car for the transportation of liquified petroleum gas or anhydrous ammonia.

A schematic of RAX 201 is presented in Figure 1. The tank car was of the order of 18.3m (60 ft.) long and 3.05m (10 ft.) in diameter.

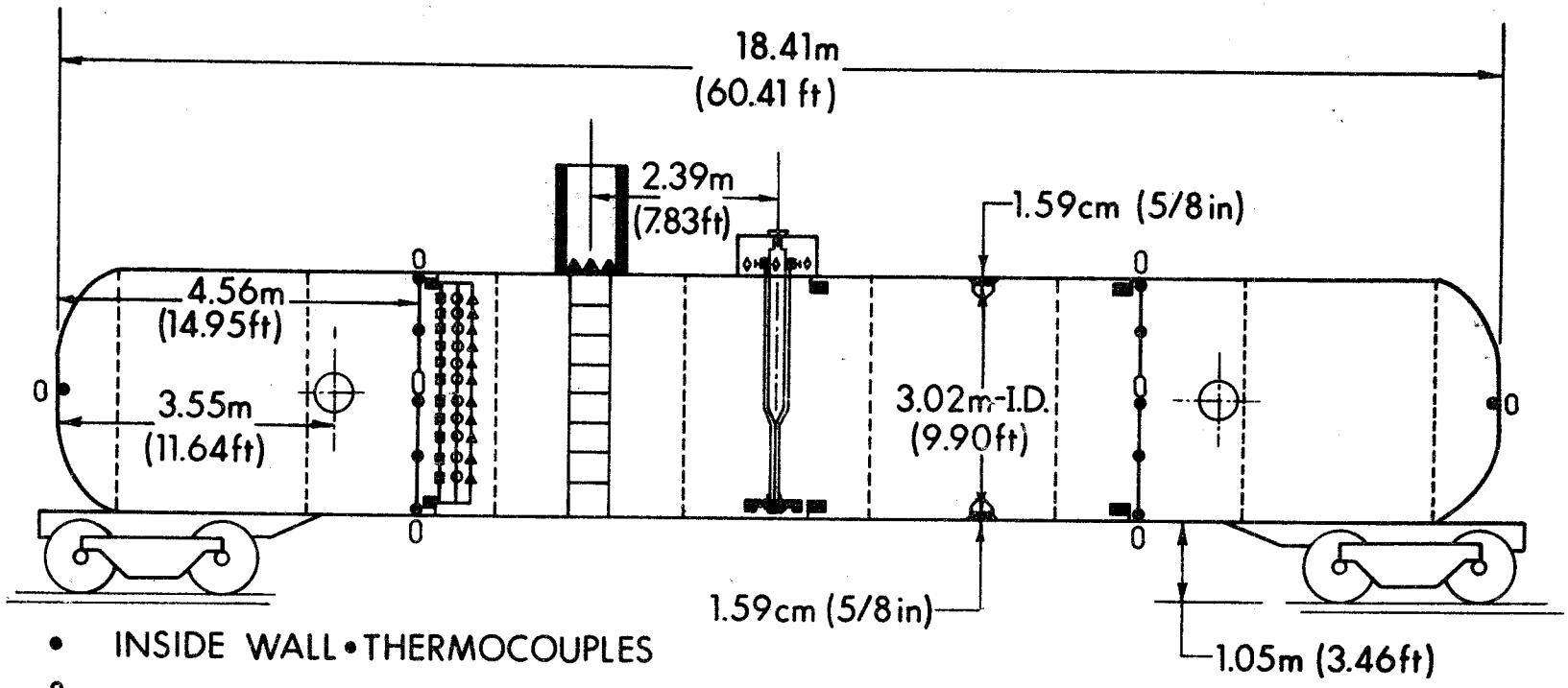

Figure 1 -Test No.8- Instrumentation Layout for RAX 201

(APPROX. SCALE: 1" = 80")

The steel shell, constructed of TC-128 steel, was 1.59 cm (5/8 in.) thick. The tank car was positioned in a large excavation which measured 45.7m in length, 30.5m in width, and 7.92m in depth (150 ft. by 100 ft. by 26 ft.). A fuel dike to contain the JP-4 fuel was constructed at the center of the excavation, and it measured 24.4m by 9.14m (80 ft. by 30 ft.). Figure 2 shows the fuel dike and RAX 201 positioned in the large excavation as they existed prior to the test.

III. FINDINGS AND ANALYSIS

A. Field Investigation

Five days after the test at WSMR, SwRI personnel arrived at the test site to examine the various pieces of the ruptured tank car in an effort to identify possible fracture initiation sites. The BRL, meanwhile, photographed and surveyed the numerous fragments. Table I is an identification list for most of the 127 fragments. These fragments consisted of the tank car, instrumentation, and the National Aeronautical and Space Agency (NASA) instrumentation stand (also referred to as the "A-frame").

Table II lists the fragments by their fragment number and their coordinate location. The distance between any two fragments can be calculated by the formula

$$D = 0.3048 \cdot \left[(X_a - X_b)^2 + (Y_a - Y_b)^2 \right]^{1/2} ,$$

where

D = the distance between item "a" and item "b" in meters,

X_a, X_b = X-coordinate of item "a" and item "b" respectively,

Y_a, Y_b = Y-coordinate of item "a" and item "b" respectively.

Figures 3 and 4 are positional maps of the fragments. Figure 3 is a scaled coordinate map of the general test area, and the fragments are listed by their fragment numbers. Figure 4, drawn to a larger scale, gives the location of the fragments in the immediate vicinity of the large excavation. Of course, the large fragments

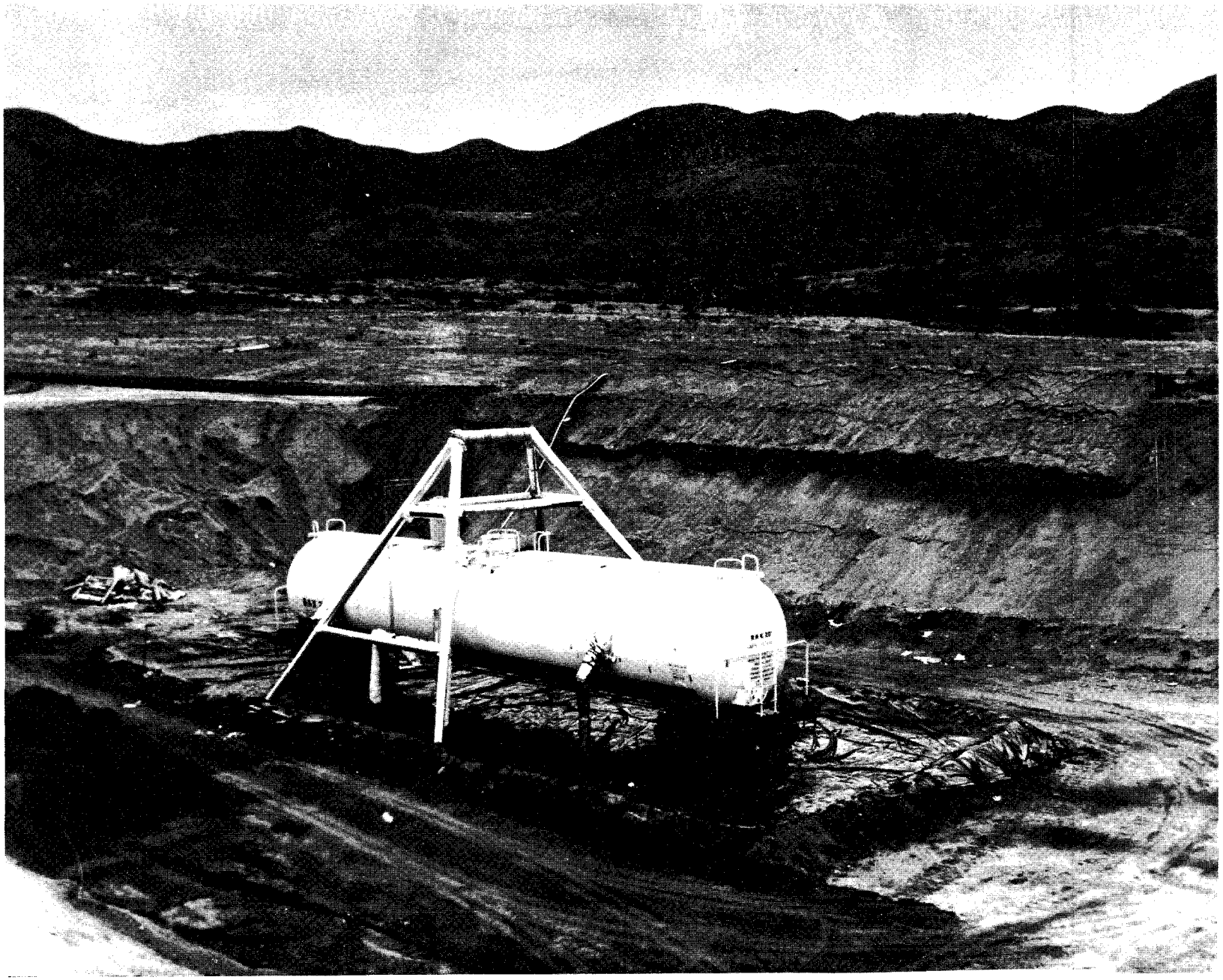

Figure 2. RAX 201 Positioned in Pit Prior to Fire Test

TABLE I

Identification of Fragments

Item No.	Identification
1	Main valve flange
2	Piece of handrail (center of car)
3	End bumper with foot step
4	East half of car shell (lettering: 173,000 201 Lt.Wt. 89900 New 9-72
5	Piece (large) of undercarriage
6	Piece of catwalk
7	Section of east end of tank
8	Air hose coupler
9	Small piece of tank shell
10	Air line valve
11	Piece of coupler
12	Section of under channel
13	West end ladder
14	Piece of handrail
15	West end of tank shell
16	Small fragment of shell 3' x 5'
17	Fill pipes (liquid) from center of tank
18	Upper most member of NASA stand
19	#1 heat flux gauge (NASA)
20	#2 heat flux gauge (NASA)
21	Jeter's slotted angle thermistor gauge
22	18" piece of catwalk
23	Jeter's wire gauge support
24	Piece of catwalk
25	LVDT support
26	Thermocouple grid from inside west end of tank
27	8' piece of catwalk grid
28	15' piece of catwalk
29	Section of railing
30	Piece of thermocouple grid from the west end of the tank
31	Piece of end of tank 3' x 5'
32	Jeter's wire gauge support
33	Leg of pot stand
34	12' piece of NASA stand
35	Upright wire conduit to Louisiana Tech relief valve

TABLE I (Continued)

Item No.	Identification
36	25' section of NASA stand
37	5' section of NASA stand
38	10" piece of under casting
39	lid of dome cover
40	Vapor vent valve pipe
41	Strap 4" x 12"
42	Other piece of strap
43	Strap
44	8' section of fill pipe-center
45	Piece of solid steel rail
46	Piece of strap (catwalk)
47	Large piece of catwalk
48	Piece of catwalk
49	Hydraulic ram for Louisiana Tech. valve
50	Hydraulic ram for Louisian Tech. valve
51	Water jacket for Louisiana Tech valve
52	Piece of catwalk
53	Thermocouple grid
54	Piece of NASA stand
55	Piece of top railing
56	****
57	6' piece of handrail
58	Portion of tank shell
59	Gauge mount; angle iron
60	Pressure gauge mount
61	Metal strap, approximately 2' long
62	Angle iron, approximately 12" long
63	Piece of catwalk
64	Piece of tank car truck
65	Hand brake wheel, bracket and chain
66	Coupler
67	Metal plate, approximately 6" x 18"
68	Small piece of truck
69	3" stainless steel tubing from shock absorbers on Louisiana Tech valve
70	Air line (brake) pipe
71	Truck and one set of wheels
72	One set of wheels
73	Gauging device (from main manway flange)

TABLE I (Continued)

Item No.	Identification
74	3" Angle valve (fill valve) from main manway flange
75	Pipe fitting
76	Tank shell
77	One set of wheels
78	Instrumentation cylinder
79	I-beam from instrumentation stand (NASA)
80	I-beam from instrumentation stand (NASA)
81	Piece of instrumentation stand (NASA)
82	Instrumentation cylinder
83	Dome housing
84	Piece of Midland valve, top housing
85	Approximately 10' section of handrail
86	9" square piece of metal, unknown
87	Settlement bowl (?)
88	****
89	Piece of Midland valve bracket
90	****
91	Air tank for brakes
92	Truck piece
93	****
94	Brake Shoe
95	Metal block, part of truck
96	Platform piece of catwalk
97	Metal casting - unknown
98	Metal block, part of truck
99	JP-4 liquid level indicator and mount
100	Rail, 2' long
101	Truck spring mount
102	Air line, 18" long
103	Pressure gauge mount
104	Piece of Midland valve - plunger or stem
105	One set of wheels
106	Concrete block for NASA stand
107	Concrete block for NASA stand
108	Concrete block for NASA stand
109	Concrete block for NASA stand
110	JP-4 liquid level float
111	Truck part
112	Rail, approximately 2' long
113	Piece of instrumentation (NASA) stand
114	Portion of Louisiana Tech relief valve
115	Truck casting

TABLE I (Continued)

Item	Identification
116	Portion of instrumentation (NASA)stand
117	South end of 30,000 gallon JP-4 fuel tank
118	Cable manhole
119	****
120	****
121	Platform piece of catwalk
122	Piece of catwalk
123	Piece of instrumentation (NASA) stand
124	Pressure gauge mount
125	Pressure gauge mount
126	Tubing (from NASA stand?)
127	****
128	Piece of instrumentation (NASA) stand

TABLE II

COORDINATE LOCATION OF FRAGMENTS

Fragment No.	X-Coordinate	Y-Coordinate	Fragment No.	X-Coordinate	Y-Coordinate
Center of Pit	444,859	219,211			
1	445,038.8	218,958.53	16	444,500.8	219,304.94
2	445,048.7	218,949.67	17	444,576.9	219,271.82
3	445,038.6	218,927.78	18	444,452.7	219,439.36
4	445,095.2	218,842.45	19	444,461.2	219,439.89
5	445,107.3	218,854.01	20	444,435.2	219,457.30
6	445,252.2	218,661.45	21	444,412.0	219,365.10
7	445,326.9	219,113.63	22	444,420.8	219,235.60
8	445,027.5	219,022.68	23	444,355.8	219,237.48
9	445,014.1	219,025.94	24	444,350.2	219,225.52
10	445,005.4	219,096.56	25	444,373.7	219,194.55
11	445,060.9	219,100.86	26	444,373.5	218,957.52
12	445,090.3	219,106.10	27	444,222.3	218,862.68
13	444,694.9	219,228.55	28	444,268.1	218,821.80
14	444,706.7	219,169.88	29	444,342.6	218,790.57
15	444,517.6	219,190.32	30	444,414.0	218,810.48
31	444,505.8	218,909.81	46	445,131.9	218,523.37
32	444,699.0	219,015.07	47	445,489.8	218,033.74
33	444,846.6	219,106.37	48	444,239.6	218,724.19
34	444,850.9	219,121.52	49	444,278.1	218,709.98
35	444,917.2	219,106.97	50	444,303.6	218,707.96
36	444,925.5	219,114.22	51	444,316.8	218,689.23
37	444,944.3	219,119.14	52	444,120.3	219,395.76
38	444,952.9	219,118.18	53	444,187.0	219,512.34
39	444,894.0	219,042.00	54	444,537.2	220,039.32
40	444,957.8	218,996.15	55	444,057.2	219,769.26
41	444,986.5	218,987.69	56	****	****
42	445,021.7	218,978.54	57	444,789.4	219,193.77
43	445,046.6	219,000.16	58	444,839.8	219,277.70
44	445,056.7	219,014.61	59	****	****
45	****	****	60	444,872.6	219,227.59

TABLE II (Continued)

Fragment No.	X-Coordinate	Y-Coordinate	Fragment No.	X-Coordinate	Y-Coordinate
61	444,889.8	219,227.47	76	444,893.0	219,173.42
62	444,903.0	219,232.44	77	444,882.2	219,169.47
63	444,943.3	219,248.89	78	444,871.2	219,160.41
64	444,948.8	219,229.65	79	444,867.1	219,154.84
65	444,954.9	219,227.84	80	444,872.7	219,152.73
66	444,959.7	219,184.67	81	444,885.5	219,155.86
67	444,980.2	219,172.89	82	444,896.2	219,145.97
68	444,985.5	219,167.97	83	444,900.5	219,143.03
69	444,963.7	219,150.96	84	444,922.1	219,146.00
70	****	****	85	444,742.4	219,152.70
71	444,940.8	219,160.72	86	444,829.3	219,194.40
72	444,923.3	219,163.96	87	444,836.4	219,201.66
73	444,908.6	219,166.94	88	444,836.8	219,206.18
74	444,905.9	219,174.96	89	444,833.0	219,211.90
75	444,902.0	219,172.75	90	444,832.0	219,216.14
91	444,833.7	219,224.73	106	444,874.2	219,198.50
92	444,847.3	219,200.53	107	444,871.0	219,233.41
93	444,850.5	219,193.85	108	444,850.1	219,231.07
94	444,845.2	219,192.10	109	444,850.4	219,193.02
95	444,856.4	219,200.73	110	444,902.7	219,189.33
96	444,858.8	219,205.58	111	444,917.9	219,176.38
97	444,861.0	219,210.04	112	444,929.9	219,179.80
98	444,860.9	219,207.41	113	444,924.0	219,174.35
99	444,887.8	219,205.31	114	444,897.9	219,158.39
100	444,891.3	219,203.81	115	444,877.7	219,172.06
101	444,878.4	219,191.00	116	444,871.0	219,195.90
102	444,871.2	219,197.70	117	444,180.8	219,397.35
103	444,860.1	219,158.86	118	444,373.8	219,075.98
104	444,839.7	219,195.91	119	444,361.8	218,879.58
105	444,838.9	219,209.43	120	444,967.1	219,157.47

TABLE II (Continued)

Fragment No.	X-Coordinate	Y-Coordinate
121	444,638.4	218,348.32
122	444,675.2	218,280.63
123	444,465.0	218,640.00
124	444,602.9	219,170.06
125	444,898.2	219,322.08
126	445,026.5	218,649.10
127	445,257.6	218,382.20
128	445,203.8	218,115.30

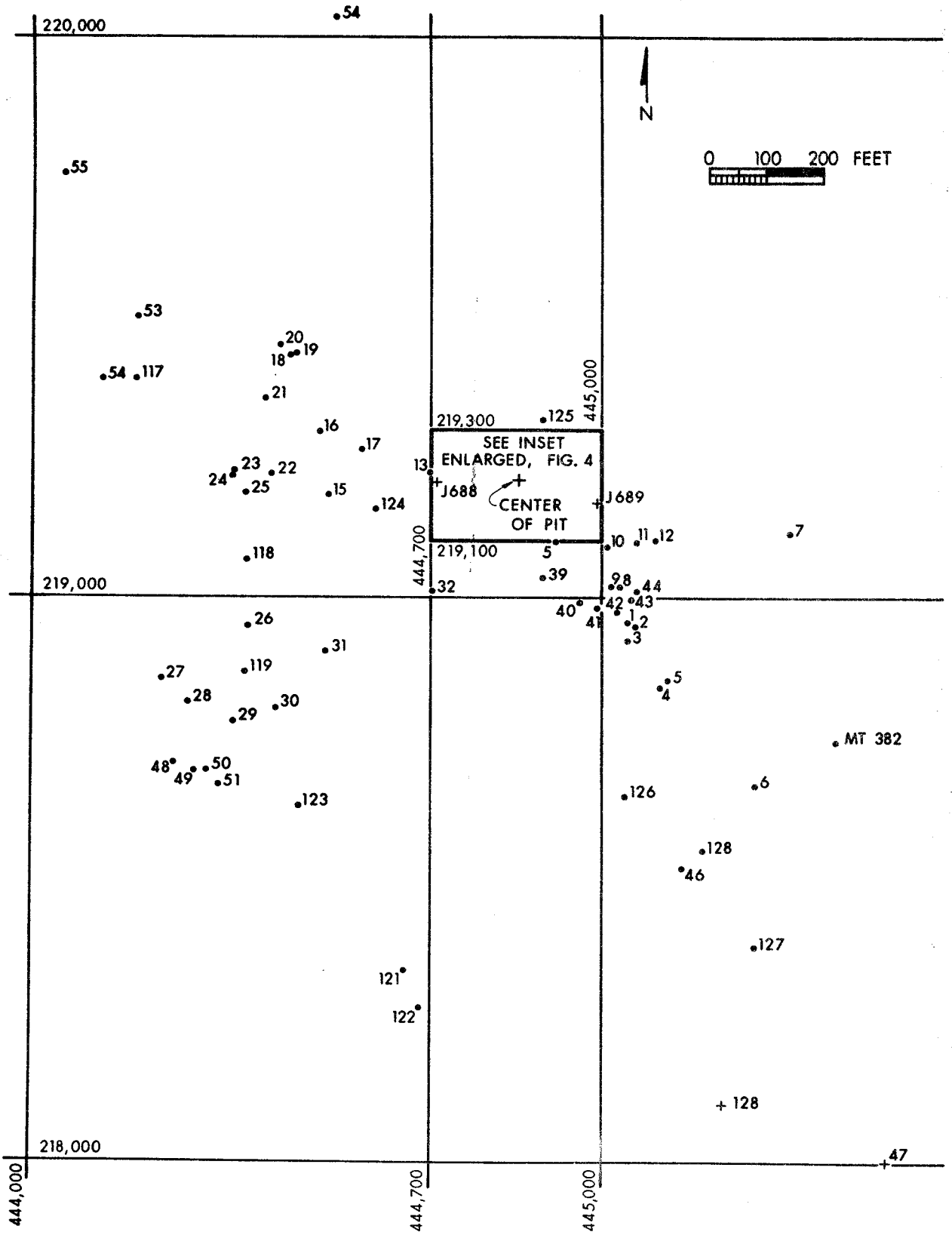

Figure 3 - Fragment Locations for Rupture of RAX 201

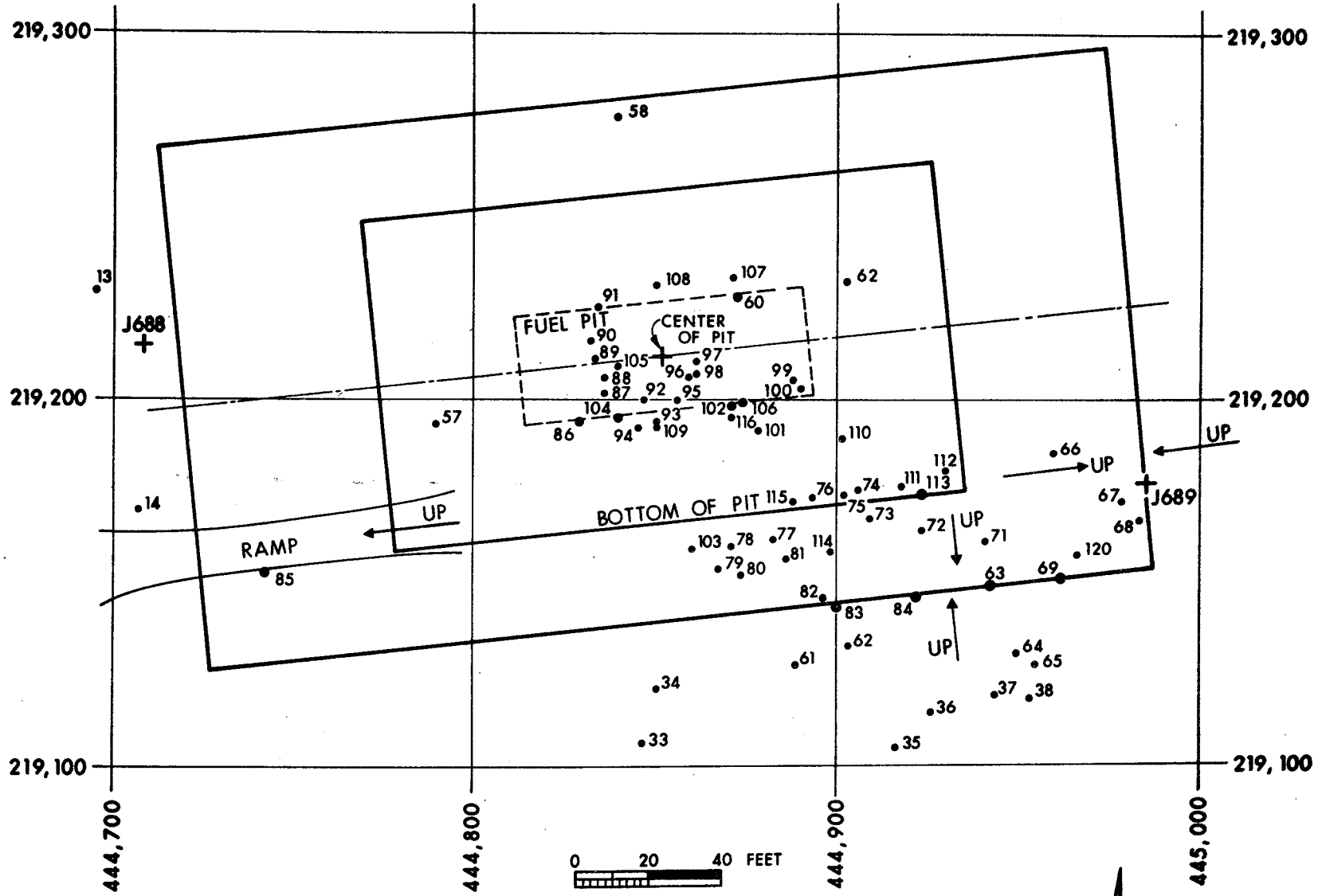

Figure 4 - Fragment Locations for Rupture of RAX 201 within Test Pit Area

occupy a finite area, so the distance measured between two points naturally depends upon where the survey stakes were placed relative to the fragments. The most distant fragment (Item 47), a large piece of the catwalk, was hurled 407m (0.25 miles) from the center of the pit.

SwRI began their examination in the test pit, the major fragments of interest being Item 76 (a portion of the tank car shell), Item 58 (a portion of one ellipsoidal head plus a piece of the shell), and Item 114 (the added manway which contained the back-up Louisiana Tech relief valve plus some of the surrounding shell).

Item 15 (a portion of an ellipsoidal head), and Item 16 (a portion of the shell), were found out of the pit to the west. These fragments were 104.2m (342.0 ft.) and 112.9m (370.3 ft.) respectively from the center of the pit. Item 4 (essentially the remainder of the shell) was out of the pit 133.4m (437.7 ft.) to the southeast. The standard manway, Item 1, containing the Midland relief valve, was located between the test pit and Item 4, 94.5m (310.0 ft.) from the center of the pit. Items 7 and 9 were originally the other ellipsoidal head. These two fragments were out of the pit 145.7m (477.9 ft.) and 73.6m (241.5 ft.), generally to the south. Table III summarizes the major tank car fragments and their distances from the center of the excavation.

Before the failure occurred, the tank car was positioned in the test pit in an east-west position - west being the end containing the entrance ramp to the large excavation. (The entrance ramp is just out of view to the left of the picture in Figure 2. That is, the east end of the car is facing the reader in Figure 2.)

By mapping the fracture paths in detail, SwRI was able to reconstruct the tank car on paper. Hence, it was concluded that Items 58 and 15 came from the west end ellipsoidal head and had been attached to Item 76. Items 7 and 9 came from the east end ellipsoidal head and had been attached to Item 4. Figures 5, 6, and 7 map out the fragment parts as they existed before the rupture. A description of each of the major fragments of the tank car is given below.

Item 76: The fracture paths bore no relationship to the long seam weld or the girth welds except that Part 76 separated from the associated ellipsoidal head very close to the shell-to-head weld for about one-half of the circumference. With the exception of one 15.2 cm (6.0 in.) long zone, all fractures were of the 45° full-shear type accompanied by some thinning typical of fast ductile fracture in a thin steel plate. The 15.2 cm (6.0 in.) long zone referred to above was located along the longitudinal fracture about 3.5m (11.5 ft.) from the head-to-shell weld. This zone was photographed, and its

TABLE III

SUMMARY OF MAJOR FRAGMENTS OF RAX 201

Item No.	Description of Item	Location	Distance from Center of Pit (M)	Distance from Center of Pit (ft)
76	Portion of Tank Car Shell	In Pit	15.4	50.7
58	Portion of Ellipsoidal Head	In Pit	21.2	69.4
114	Added Manway	In Pit	19.9	65.4
15	Portion of Ellipsoidal Head	West of Pit	104.2	342.0
16	Portion of Tank Car Shell	West of Pit	112.9	370.3
1	Standard Manway	Southeast of Pit	94.5	310.0
4	Portion of Tank Shell	Southeast of Pit	133.4	437.7
7	Portion of Ellipsoidal Head	South of Pit	145.7	477.9
9	Portion of Ellipsoidal Head	South of Pit	73.6	241.5

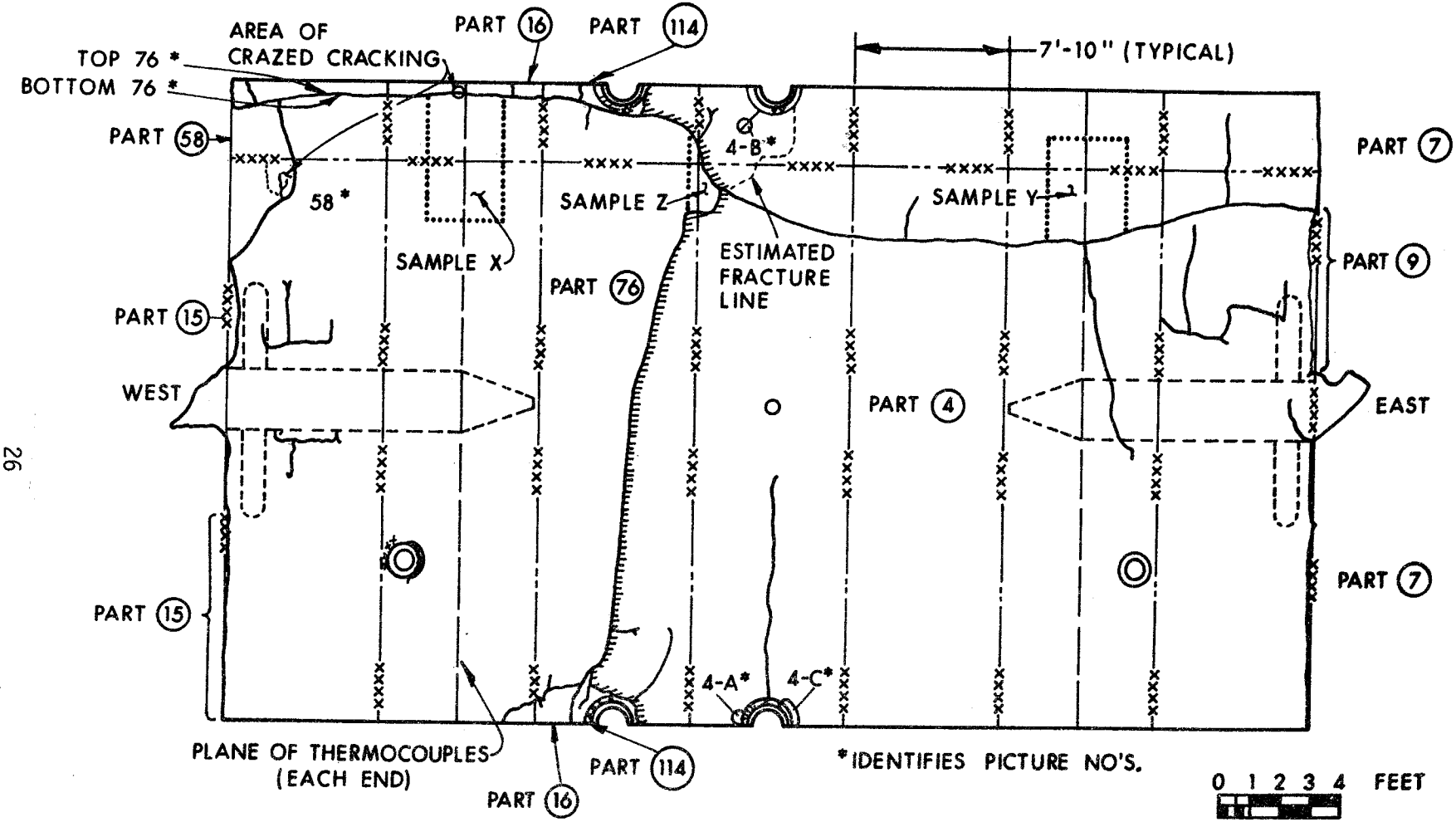

Figure 5 - Fragments of Ruptured Tank Car Assembled as They Existed Before Rupture

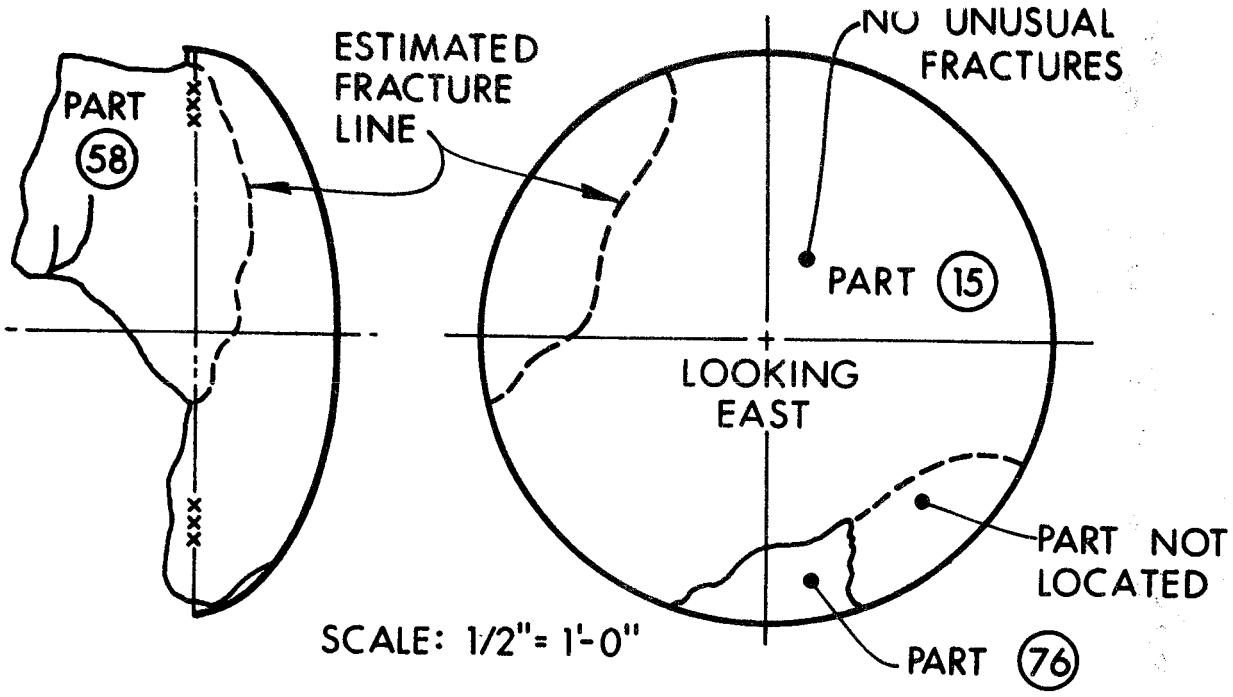

Figure 6 - West End View of Fragments as They Were Positioned Before Rupture

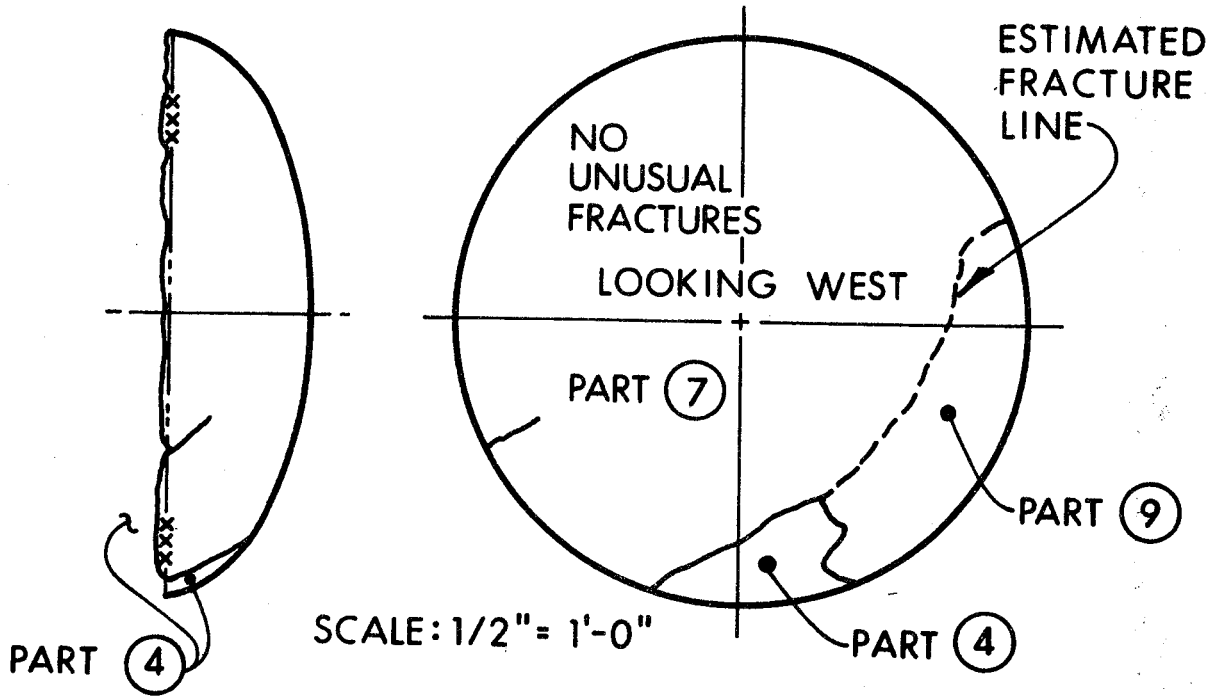

Figure 7 - East End View of Fragments as They Were Positioned Before Rupture

characteristics are as follows:

(1) A series of secondary cracks, parallel to the fracture surface, were located in an area approximately 2.54 cm (1.0 in.) wide on each side of the fracture surface;

(2) The fracture surface was coarse and irregular, typical of intergranular fracture, and was oriented 90° to the shell plate surface;

(3) There was very little reduction in shell thickness at the midpoint of this zone, but an exaggerated reduction - approximately 1.19 cm (0.47 in.) from the nominal 1.59 cm (0.625 in.) - was observed at each end of the zone as the fracture surface converted to a 45° shear.

These conditions are characteristic of a stress-rupture failure under the conditions of loading which existed and therefore, this zone is a prime suspect as the fracture initiation point.

Item 58: The fracture paths bore no relationship to the portion of the shell-to-head weld which it contained. The fractures were typically 45° shear except for one small area near the end of one secondary crack. This area, which was also photographed, was characterized by one parallel secondary crack near the fracture surface, the latter being generally normal to the plate surface. Although this indicates the possible beginning of a stress-rupture type of failure, the general location would indicate that this zone is not likely to be the point of initiation of the tank car failure. This point will be discussed in more detail after the description of major fragments has been completed.

Item 114: The fracture path around the manway appeared to be confined to the shell plate material and was essentially all 45° shear fracture.

Item 4: The relationship of fragment paths and weld seams were similar to those described for Item 76. Except for the portion of the fracture paths that circled the standard manway and those that could not be seen, the fracture surfaces were all characterized as 45° shear. Item 4 was exceptionally twisted and bent on one end (adjacent to Item 76) which made it difficult to map and examine the fracture surfaces. It is not known if this deformation occurred at the time of failure or on impact at the landing point. A large hole in the ground near the point of impact, and the fact that some of the edges were buried in the ground, indicates that some deformation must have occurred on impact.

Items 7, 9, and 15: The fracture paths did not appear to have any significant relationship to the shell-to-head weld and were generally of the 45° shear type of fracture.

Item 16: The fracture paths had no relationship to the girth weld which it contained and the fracture surfaces were characterized by the 45° shear type of fracture.

Item 1: The manway separated from the shell at the manway-to-shell weld and therefore was not characterized by 45° shear fracture. Since the main longitudinal fracture paths were a meter or so away from this manway, it does not appear likely that the tank car failure initiated in the region adjacent to the manway.

B. Conclusions of Field Investigation

The relative positions of the major fragments would indicate that the failure initiated somewhere in the west end of the car. This conclusion is deduced from the fact that the two major pieces of the cylindrical portion of the tank (Items 4 and 76) were displaced east of their original location. Item 76 was displaced a few meters from its original position while Item 4 was displaced approximately 133.4m (437.7 ft.) southeast of its original position. The lack of any unusual fracture surfaces in Items 4, 7 and 9 support this conclusion.

The prime candidate as the point of initiation appears to be a 15.2 cm (6.0 in.) long zone along the main longitudinal fracture path 3.5m (11.5 ft.) from the west head-to-shell weld. A stress-rupture type of failure is suspected.

The only other zone having an unusual fracture appearance is positioned four feet circumferentially away from the main longitudinal fracture path and therefore would not appear to be the point of initiation since the hoop stress is nominally twice the axial stress in a cylindrical vessel.

C. Metallography Investigation

A limited metallurgical investigation of the particular plate in which the fracture was thought to have initiated was undertaken by SwRI. Several samples of steel were removed from the ruptured tank car by the BRL and sent to SwRI. The locations of the sample materials sent, labelled X, Y, and Z, are shown in Figure 5. However, sample material X was the particular plate of interest.

Ten tensile/stress-rupture specimens were machined from sample X at the end opposite the fracture path. In addition, one metallurgical specimen was removed from this area. Also,five metallurgical specimens were taken from sample X along the fracture path.

The tensile and stress-rupture tests were run at 482.2°C (900°F), 565.6°C (1050°F) and 648.9°C (1200°F) in a servo-controlled hydraulic universal testing machine. The specimens were full-plate thickness, 1.588 cm (0.625 in.), with a 0.635 cm by 2.54 cm (0.25 in. by 1.0 in.) gage section and they were oriented circumferentially relative to the tank car body. The results of these tests are presented in Table IV.

The tensile and stress-rupture test data were analyzed parametrically by the method of Larson and Miller:

$$P = T\ (20 + \log \tau) \cdot 10^{-3},$$

where

P = Larson-Miller parameter,

T = Temperature (°F),

τ = Lifetime (hours).

The tensile data were plotted at an assumed life of 0.03 hours and the stress-rupture data were plotted at their actual rupture lives in Figure 8.

The Larson-Miller curve, Figure 8, was used to predict the stress-rupture strength of the tank car material at several combinations of temperature and rupture life as shown in Table V. These data are converted with the hoop stress formula,

$$PD = 2\ \sigma t$$

where:

P = rupture pressure (dyne/cm^2),

D = hoop diameter (cm),

σ = stress (dyne/cm^2),

t = thickness of steel (cm).

TABLE IV

ELEVATED TEMPERATURE TEST RESULTS ON TANK CAR STEEL

Spec Ident.	Temperature (^{o}C)	Temperature (^{o}F)	Stress (10^{8} · dynes/cm^{2})	Stress (10^{3} · lbs/in^{2})	Time to Failure (min)	Elongation (%)
9T	482.2	900	52.9	76.7	(a)	31.1
9AS	482.2	900	42.7	62.0	244	21.5
9BS	482.2	900	45.0	65.2	16	24.7
10T	565.6	1050	41.4	60.0	(a)	29.8
10AS	565.6	1050	34.0	49.3	52	22.6
10BS	565.6	1050	28.8	41.8	138	16.3
12T	648.9	1200	33.6	48.7	(a)	24.7
12AS	648.9	1200	21.0	30.4	36	22.4
12BS	648.9	1200	13.7	19.8	115	23.5
S	648.9	1200	22.1	32.1	6	(b)

(a) Tensile Test

(b) Data not reported

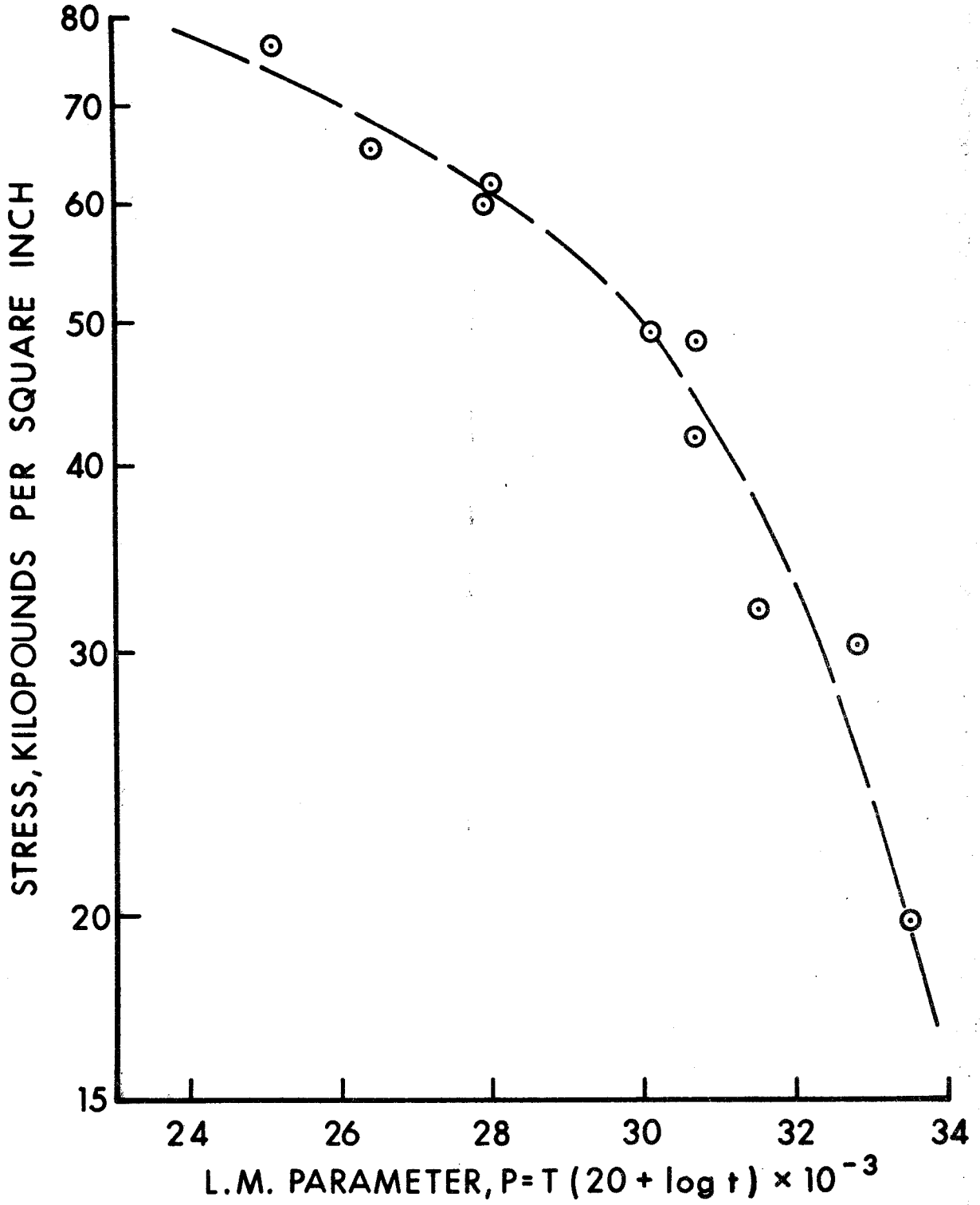

Figure 8 - Parametric Analysis of Tensile and Stress Rupture Data

TABLE V

STRESS-RUPTURE STRENGTHS OF TANK CAR STEEL

Temperature (^{o}C)	Temperature (^{o}F)	Stress for Time-to-Rupture[a] 0.2 hr	0.5 hr	1.0 hr	2.0 hr
482.2	900	48 (69)	46 (67)	45 (65)	43 (63)
565.6	1050	38 (55)	36 (52)	34 (49)	31 (45)
648.9	1200	23 (33)	19 (27)	15 (22)	12 (18)

(a) Units are 10^{8} · dynes/cm^{2} (10^{3} · lb/in^{2})

Therefore, Table VI, using the hoop stress formula, predicts the tank car pressure which would cause rupture at the same temperature-time combinations.

The pressure-time and temperature-time data obtained during the full-scale test were combined to develop a pressure-temperature history curve in Figure 9. The thermocouple located nearest the point where the fracture was believed to have been initiated (the 12:00 wall thermocouple located at the west end grid-wall thermocouple plane) was used to obtain the temperature-time curve. Therefore, depicted in Figure 9 are:

(1) the pressure-temperature history curve of the full-scale tank car test;

(2) the tensile strength of tank car material as a function of temperature;

(3) the 0.2-hour and 0.5-hour stress-rupture strengths of the tank car material as a function of temperature;

(4) the tensile "design curve" of burst pressure of the tank car versus temperature (from AAR).

Examination of Figure 9 indicates that the tensile strength of the tank car was higher than the "design" curve. In addition, the time dependence of high temperature strength properties reduces the pressure at which tank rupture would be predicted. Note that the tank car ruptured just below 650°C (1200°F) at a pressure stress equivalent to the predicted 0.5 hour stress-rupture strength of the tank car material. All evidence thus confirms the original conclusion that the material failed by stress rupture.

The metallurgical examination of the suspected fracture initiation area revealed that the general microstructure was pearlitic plus blocky ferrite, Figure 10. An unexpected observation was the presence of a thin layer, 0.102 cm (0.040 in.) maximum, of an acicular microstructure (see Figure 11) on the inside diameter tank surface where the fracture was thought to have initiated. A hardness traverse across this layer into the normal microstructure (Table VII) indicated that the layer had been tempered at a high temperature after it was formed, indicating that it was formed before the fire test. No evidence of this condition was found at the other end of Sample X where the tensile/stress-rupture specimens were located.

TABLE VI

TIME-to-RUPTURE AT VARIOUS TANK CAR PRESSURES[a]

Temperature (^{o}C)	Temperature (^{o}F)	Pressure for Time-to-Rupture[b] 0.2 hr	0.5 hr	1.0 hr	2.0 hr
482.2	900	514 (730)	493 (700)	479 (680)	465 (660)
565.6	1050	410 (580)	390 (550)	369 (520)	334 (470)
648.9	1200	252 (350)	203 (280)	169 (230)	141 (190)

(a) Assuming:

Tank Dia. = 301.62 cm (118.75 in)

Tank Wall = 1.638 cm (0.625 in)

(b) Units are

10^{5} · dynes/cm^{2} (lbs/in^{2} gauge)

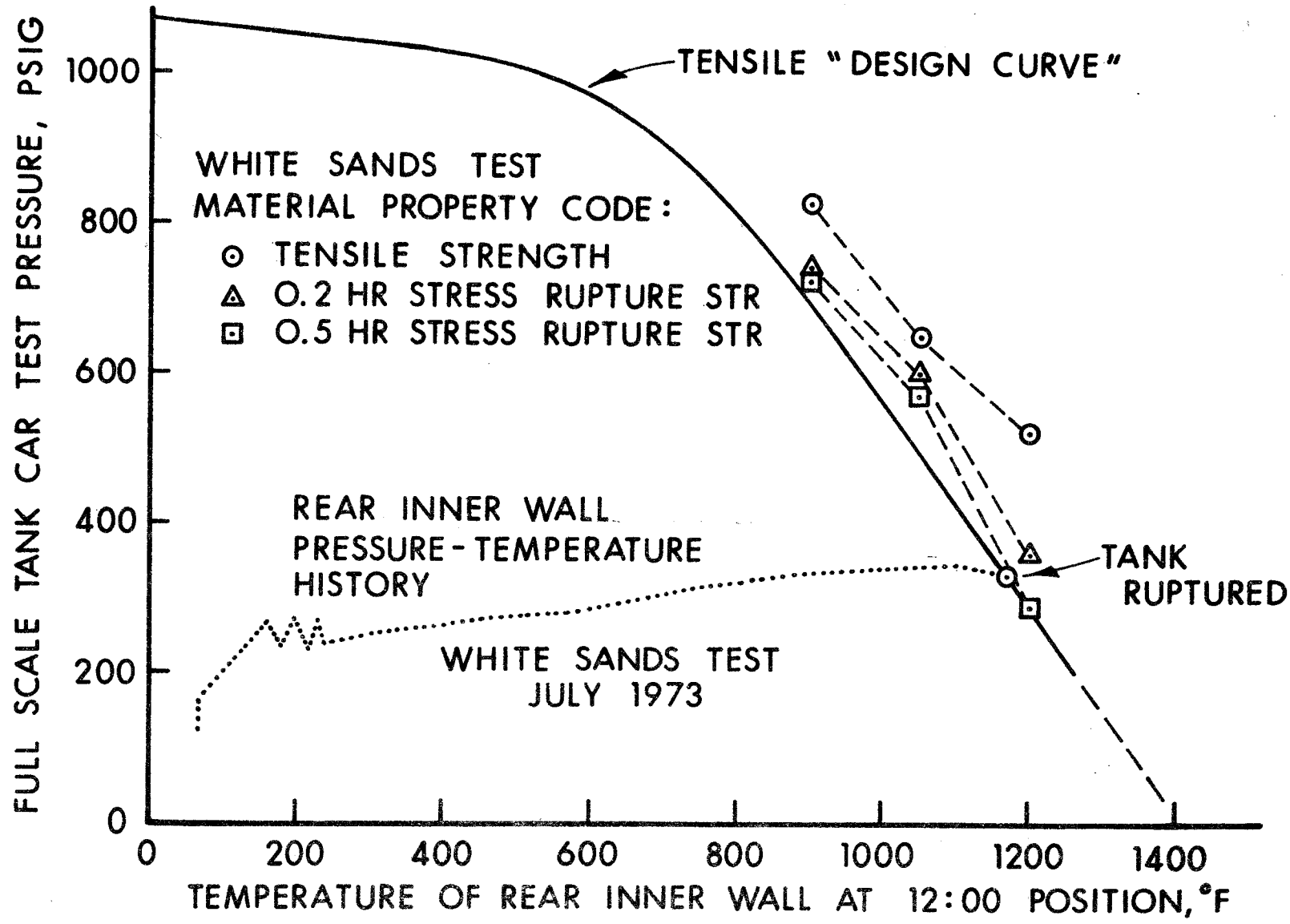

Figure 9 - Comparison of Test Conditions with Material Properties

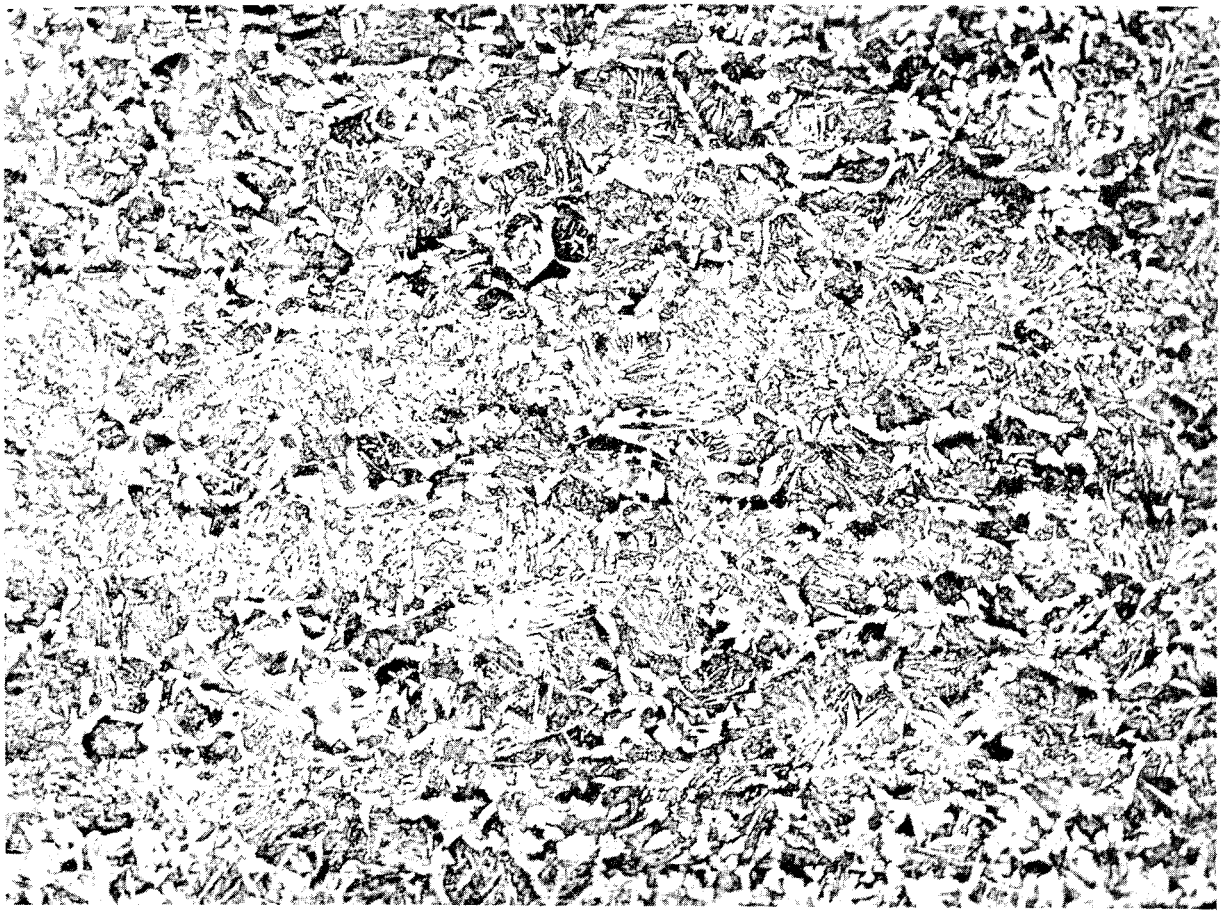

100X Plate 20117 Nital

Figure 10. Typical Microstructure of Tank Car Material

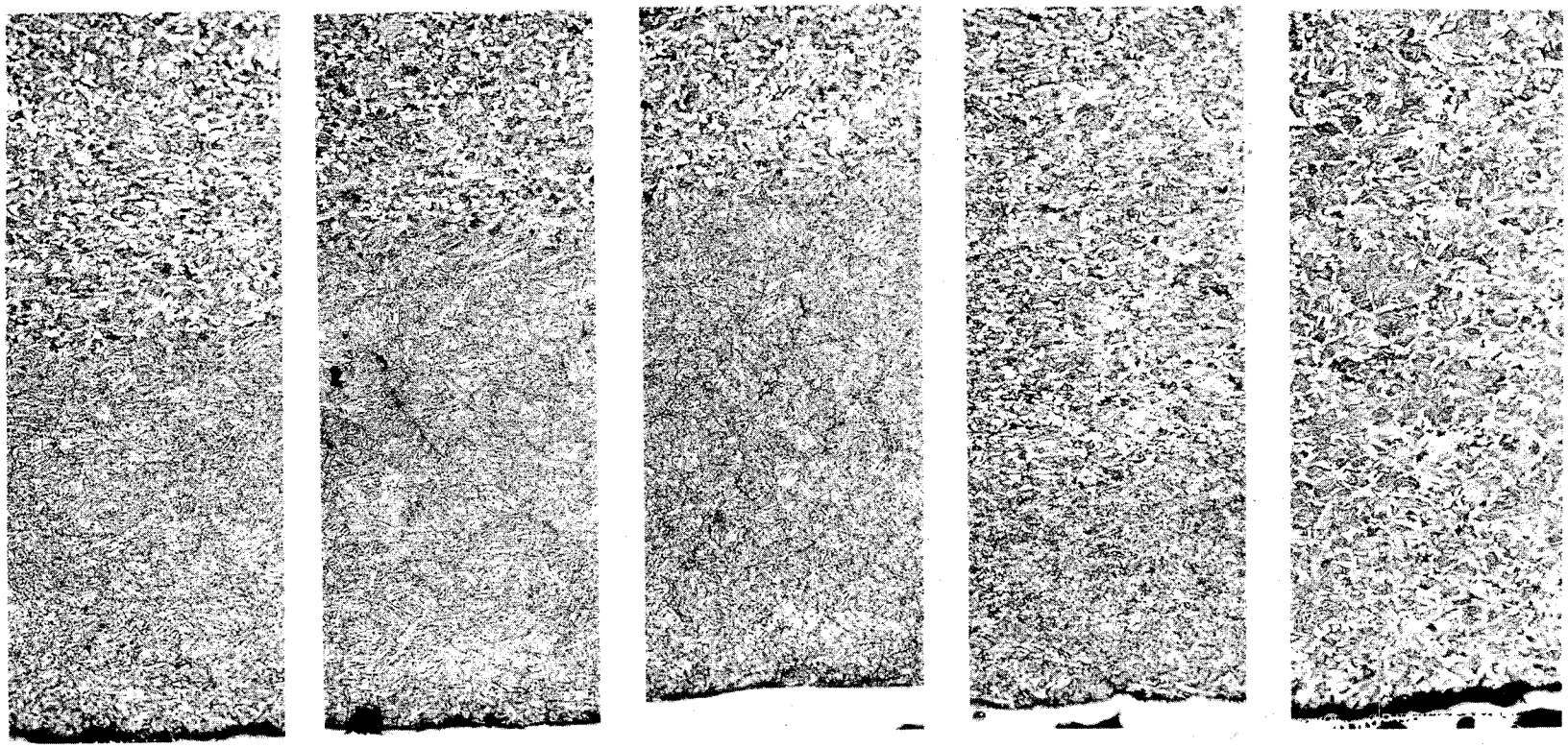

Plate 20120
75X

Plate 20119
75X

Plate 20125
75X

Plate 20126
75X

Plate 20127
75X

Figure 11. Variation in Depth of Acicular Microstructure
Along Fracture at Suspected Initiation Site (I.D.Surface)

TABLE VII

HARDNESS DATA TAKEN ON SECTION 3-3

Indent. No.	Location	Knoop Hardness[a]	Rockwell B Hardness[b]
1	Trans.[c]	221	94
2	"	232	96
3	"	232	96
4	"	223	94
5	"	221	94
6	Norm.[d]	209	92
7	"	209	92
8	"	211	92
9	"	230	96
10	"	204	91

(a) 500 gm load, 20X eyepiece

(b) Converted from Knoop hardness

(c) Transformation microstructure near I.D.

(d) Normal microstructure

The acicular type of microstructure is produced by heating above 732°C (1350°F) followed by relatively fast cooling. Considering the conditions existing during the tank car test, it is difficult to imagine how a thin layer on the inside diameter surface would reach a higher temperature than the body of the steel. In consideration of this and the hardness traverse data, it appears unlikely that the layer was produced during the test. One can only assume, therefore, that the condition existed in the steel plate as received, or that it was produced during tank car fabrication or tank car instrumentation. Since the spot appears to be quite limited in extent, one possible explanation would be a rapid, localized heating from the inside diameter surface with a torch, such as might have been used in the application of the copper beads (which were installed on the inside walls to house the thermocouples) or bracket mounts (which were installed for the pressure gauges and grid network).

The tank car fracture appeared to initiate within the acicular microstructure; in fact, several secondary cracks were observed to arrest at the boundary between the acicular and normal microstructures, Figure 12. However, based on limited stress-rupture data, the normal material would have failed by stress rupture in a rather short additional time had the acicular layer not been present.

IV. SUMMARY

All evidence supports the conclusion that a stress-rupture failure initiated in the west end of the tank car, near the top of the car. The prime candidate as the point of initiation appears to be a 15.2 cm (6.0 in.) long zone along the main longitudinal fracture path 3.5m (11.5 ft.) from the west head-to-shell weld. This zone is marked in Figure 3 as "area of crazed cracking," located just to the top of the Sample X in the diagram. The tank fracture appeared to initiate within a region where there was a thin layer of an acicular microstructure. Due to the very close proximity to the plane of the thermocouple, this condition was probably caused by the heat required to install instrumentation brackets or holders. However, the normal material would probably have failed by stress rupture at approximately the same time (within several minutes) had the acicular layer not been present.

Finally, tensile tests showed that the time dependence of high temperature strength properties of the steel reduces the pressure at which rupture would be predicted. That is, the longer the tank car is subjected to high temperatures, the lower the pressure that is required to rupture the vessel.

100X Plate 20129 Nital

Figure 12. Secondary Crack on Tank Car I.D.Surface Arresting at Microstructure Interface